



APPLICATION OF REMOTE SENSING IN LITHOLOGICAL DISCRIMINATION OF PRECAMBRIAN BASEMENT ROCKS OF ZUNGERU AREA, PART OF SHEET 163 (ZUNGERU NW), NORTH CENTRAL NIGERIA.

¹Aliyu, Abubakar Eneye, ⁴Adamu, Lukman Musa, ⁵Abdulmalik, Nana Fatima, ²Amuda, Abdulgafar Kayode, ³Umar, Aliyu Ohiani, ⁶Umar Nazif, and ¹Jungudo, Salihu Muhammad

¹Department of Geology, Ahmadu Bello University, Zaria, Kaduna State, Nigeria

²Department of Geology, Bayero University Kano, Kano State, Nigeria

³Department of Geology, University of Maiduguri, Maiduguri, Borno State, Nigeria

⁴Department of Earth Sciences, Prince Abubakar Audu University, Ayingba, Kogi State

⁵Centre for Energy Research and Training, Zaria, Nigeria

⁶Nigeria Geological Survey Agency, Abuja, Nigeria

*Corresponding author's email: grunerite7@gmail.com

ABSTRACT

Remote sensing technology has advanced significantly, making it useful for geological applications such as structural and lithological mapping, as well as mineral prospecting and mapping. This study looks at how certain enhancement techniques on Landsat 7 ETM+ data can be used to map surface geology, resulting in color composite imagery that can be interpreted and validated through field mapping exercises. Because some of these rocks are poorly exposed and some portions of the research region are inaccessible, field mapping was supplemented by remote sensing lithological mapping techniques. False Color Composite images for bands (7:4:1 and 7:5:4), Principal Component analysis (PC1, 2, 3 and PC4, 5, 6) and RGB composite images of Landsat band ratios (1/3:5/7:3/5 and 5/1:5/7:4) proved useful in determining the approximate boundaries of the various lithology in the research area. Gneiss and quartzites occur in the central and western quadrants of the study area, mylonites and schist in the eastern quadrant, and amphibolite in the southern and southeastern quadrants, according to GPS sample locations of the individual rock types found in the study area plotted on the processed images. The contact relationships between these rocks are mostly gradational and interlayered. As a result, a thorough examination of satellite optical imagery, such as Landsat data, can greatly aid lithological inquiry and the creation of more detailed geological maps in areas that are inadequately understood.

Keywords: Band Ratio, False Colour Composite images, Landsat 7 ETM+, Principal Component Analysis

1.0 INTRODUCTION

Nigeria is underlain by Precambrian Basement rocks, Jurassic anorogenic Younger Granites, Cretaceous to Recent sediments, and Tertiary to Recent volcanic rocks, with the basement rocks accounting for over half of the country's land mass (Black, 1980). The study area is in and around Zungeru, Niger State, Nigeria's north central region. It is located within 9°45' and 10°00' N, and 6°00' and 6°15' E, and is part of Zungeru (Sheet 163NW), which covers an area of approximately 770 km².

Geological mapping at all scales is one of geologists' principal goals. There are, however, certain drawbacks to geological field mapping and mineral exploration. Inaccessibility, insecurity and social instability, inadequate outcrop exposures, and so on are some examples of these limitations. In addition, conventional geologic field mapping methods are costly and time-consuming compared to remote sensing techniques and approaches, especially for vast areas (Abdelmalik, 2018).

Earth sciences, geography, archeology, and environmental sciences have all benefited from remote sensing technologies. Earth scientists have employed remote sensing data to look at worldwide experiences in environmental geology, mineral exploration, and hydrocarbon exploration (Kucukkaya 2004;

Hellman and Ramsey 2004; Galvao et al., 2005; Watts and Harris 2005; Vaughan et al. 2005; Aminzadeh and Samani, 2006; Lammoglia and Filho 2011; Shi et al., 2012; Petrovic et al. 2012; van Ruitenbeek et al. 2012). For decades, remote sensing techniques have been utilized successfully for geological mapping and mineral exploration (Amer et al., 2010; 2012; Zhang et al., 2007).

Many studies have shown that remotely sensed data can be used to update an area's current maps (Chorowicz and Ragin, 1982; Ferradini, Cornee and Simon, 1993). Many of the disparities discovered between published maps and those produced from satellite images were determined to be attributable to omissions or inaccuracies in field geological mapping, as evidenced by succeeding field study. A range of criteria (such as overall geologic context, weathering, landforms, drainage, structural features, soil, vegetation, and spectral properties) obtained from remote sensing data are used to identify broad lithological contacts.

The present study aims to create the geological map of Zungeru by applying different image processing techniques for Landsat ETM+ satellite data in order to discriminate between the varieties of rock type. Landsat ETM+ imagery were examined

using optimization techniques like band ratios, color composites, and principal component analysis (PCA). Different lithologic units in the study area were mapped using visual interpretation, verified with ground-truth data, and combined using a geographic information system with the aid of these enhancing techniques.

2.0 GEOLOGICAL SETTING

2.1 The Nigerian Basement Complex

The Nigerian Basement is a component of a mobile belt located in between the Congo and the West African Cratons (Fig.1).

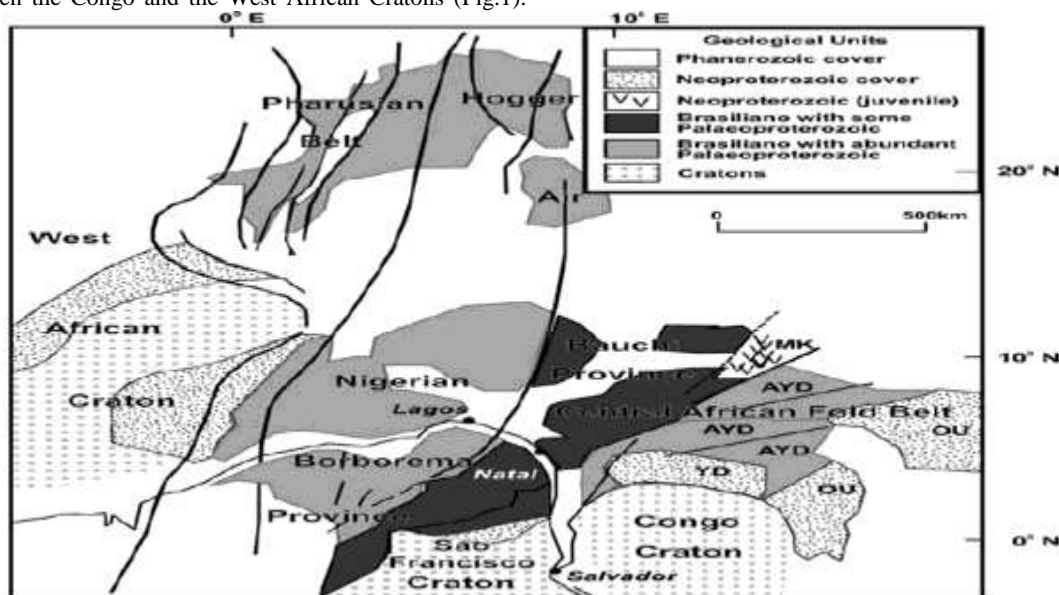


Fig. 1: The location of the Nigerian Basement Complex in reference to the provinces of Hoggar and Borborema (adapted from Dada, 2008).

The Migmatite Gneiss Complex (MGC), the metasedimentary belts, and the Older Granites are the three major lithologic units that make up Nigeria's basement complex.

The Migmatite-gneisses complex is commonly recognized as the basement stricto sensu (Rahaman, 1988, Dada 2008). It is a heterogeneous assemblage comprising migmatized gneisses, orthogneisses, paragneisses, and a variety of metamorphosed basic and ultrabasic rocks with a metamorphic facie grade of mostly upper amphibolites (Dada 2008). Understanding the crustal evolution of the Migmatite Gneiss Complex is complicated by a dearth of geochronological data (Kroner et al., 2001).

The N-S trending syn-formational metasedimentary belts are restricted to the western Nigeria. The basement complex of western Nigeria has been divided into twelve distinct metasedimentary belts (Ajibade et al., 1987; Turner, 1983). They are mostly upper green schist to lower metamorphosed amphibolites that resemble the Archean greenstone belt. They include Zungeru-Birnin Gwari, Kushaka, Malumfashi, Kazaura, Wonaka, Maru, Anka, Zuru, Toto, Iseyin-Oyan River, Ife-Ilesha and Igara-Kabba-Lokoja belts (Turner 1983; Danbatta 2008). Psamatic schist, pelitic and semipelitic schist, metasandstone, metaconglomerate, quartzite, marble, mafic to ultramafic rocks, acid to intermediate volcanic rocks, calc-silicate rocks, and

Plate tectonic events are believed to have formed the belt around 600 Ma, when the passive continental continental margin of the West African Craton collided with the active continental margin of the Tuareg Shield (Burke and Dewey, 1972; Leblanc, 1981; Black et al., 1979; Caby et al., 1981; Ajibade et al., 1987; Garba, 2002). The Nigerian Basement is located in the belt's reactivated segment (Ajibade et al., 1987). The Nigerian Basement evolved through polyphase tectono-metamorphic history, including Liberian (2700±200 Ma), Eburnean (2000±200 Ma) and Pan-African (600±150 Ma) events (Grant, 1970; Ajibade et al., 1987; Dada 1998).

banda iron formations are among the most common lithologies (Turner 1983; Danbatta 2008).

The syn-collisional to post-collisional granitoids constitute the Older Granite suites. They intrude both the migmatite-gneiss complex and the metasediments. Rocks ranging in composition from granite to tonalite and charnockites with minor deposits of syenite, gabbro, and pegmatite make up the granitoids (Ajibade et al., 1987). The radiometric dates of the granitoids are in the 750-500 Ma range, which is within the Pan-African spectrum. To differentiate them from Mesozoic orogenic granite ring-complexes (the Younger Granites), these Pan-African granitoids are referred to as the Older Granites in Nigeria.

3.0 MATERIALS AND METHODS

Remote sensing interpretation, field studies, and laboratory analyses are all part of the approach used in this research. Remotely sensed multispectral datasets including LANDSAT Enhanced Thematic Mapping (ETM+) imageries were processed. These Landsat bands (1, 2, 3, 4, 5, & 7) were downloaded from the Global Land Cover Facility's website (<http://glcf.umd.edu/>). Using ENVI 4.5 software, these images were calibrated and refined to create color composites, employing image processing techniques such as false color composite, band rationing, and principal component analysis.

The colors red, green, and blue (RGB) were chosen as the primary colors in these basic image processing techniques to emphasize the disparities between lithologies. A geological mapping exercise (ground truthing) which entails detailed observation of the various rock types in the field was used to confirm the accuracy of the results.

Field investigation was conducted in two(2) phases: the first was a five-day reconnaissance visit, followed by a two-week field camping period during which geological field mapping of the studied region was carried out on a scale of 1:50,000. Fresh rock samples were taken and the Location information of each sampling spot was recorded with the aid of a Global Positioning System (GPS). Representative rock samples were chosen from various rock types, and thin sections (slides) were created in the thin section laboratory of the department of geology, Ahmadu Bello University. Under a petrological microscope, the slides were inspected for minerals and other properties that had not before been seen in hand specimens.

4.0 RESULTS AND DISCUSSION

4.1 FALSE COLOUR COMPOSITE TECHNIQUE

For lithological mapping of rocks, false color composite techniques such as those used by Rowan et al.(1974), Raine et al.(1978), and Riley et al.(2006) were utilized, displayed in R:G:B. False color composites (FCC) are utilized to emphasize geologic features for visual examination (Gad and Kusky, 2007; Massironi et al., 2008; Qari et al., 2008). Up to three bands or ratio images have to be chosen in a false color composite method based on known mineral absorption properties. Visual analysis aids in the selection of optimal band combinations for more complex computational techniques, as well as providing a preliminary indication of the likelihood of mapping the chosen lithologies.

In fig. 2, false colour composite image for bands 7, 4, 1 displayed in R.G.B, the red and green colours are indicating different rock types and vegetation, while the blue colour delineates the major river in the southeastern quadrant of the map. The very dark reddish-purple colour at the eastern portion of the map is area occupied by both amphibolites and schist. Gneiss is represented at the central and northeastern portion of the map by light reddish-purple colour. The remaining rock types and vegetation in the area are represented by green colour. Fig. 3 depicts areas covered by gneiss, amphibolites, migmatites and mylonites by yellow colour while vegetation appears as blue.

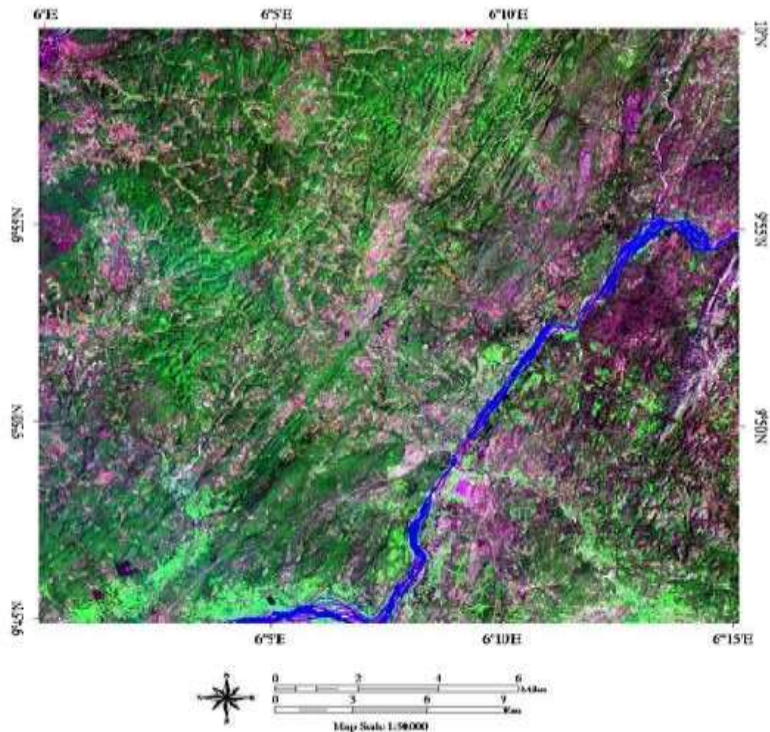


Fig. 2: False colour composite image for bands 7, 4, 1 displayed in R.G.B.

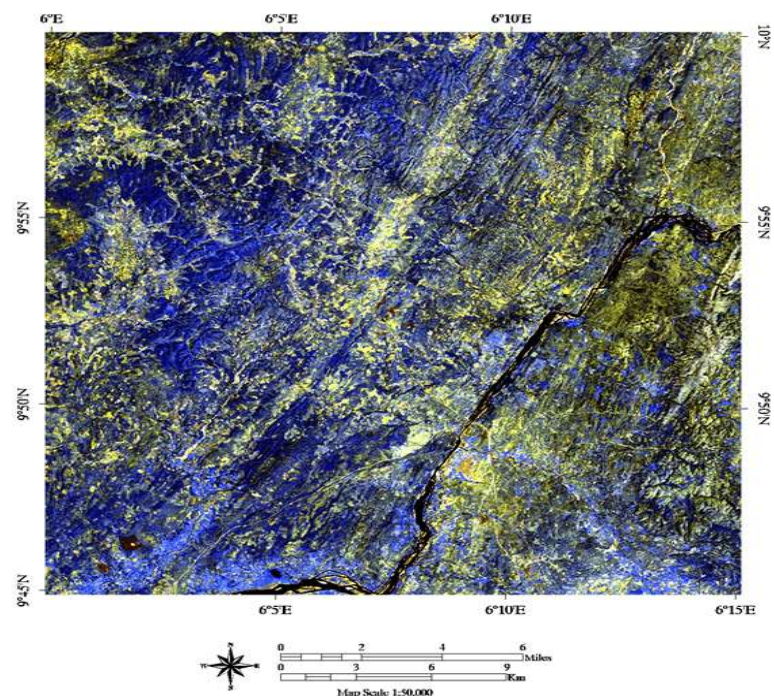


Fig. 3: False colour composite image for bands 7, 5, 4 displayed in R.G.B.

4.2 BAND RATIONING

In multispectral and hyperspectral images, band ratio is a very useful method for highlighting features. A specific mineral

potential could be mapped using the band ratio technique based on the absorption feature characteristics of the individual minerals. The R.G.B composited image and the Landsat band ratio both performed a key role in recognizing distinct rock types in the research area. Band ratios are more effective than single bands for distinguishing changes induced by geographic features and scene illumination conditions, especially when they are generated by integrating three ratio images in the red, green, and blue bands. The band ratio image methodology is carried out by dividing the digital number (DN) values of one band by the associated DN value of another band and displaying the resultant DN values as gray scale images (Sabins, 1997).

False colour composite in R.G.B of band ratio 1/3:5/7:3/5 (fig. 4) displays amphibolite and gneiss as blue while quartzite generally exhibit as greenish-yellow colouration. The major water body in the southeastern portion of the area is displayed as black while areas occupied by gneiss and amphibolites are light purple (fig. 5).

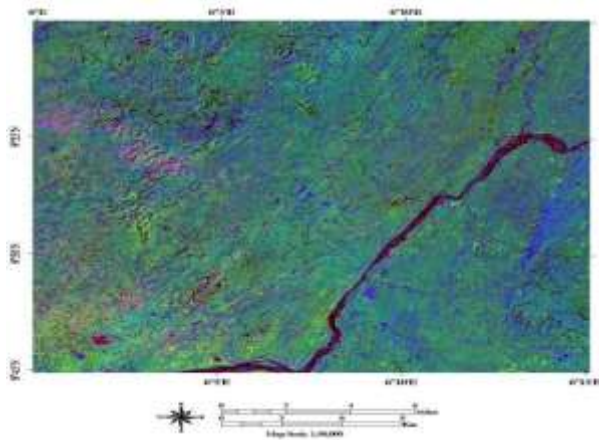


Fig. 4: False colour composite image for bands 1/3:5/7:3/5 displayed in R.G.B.

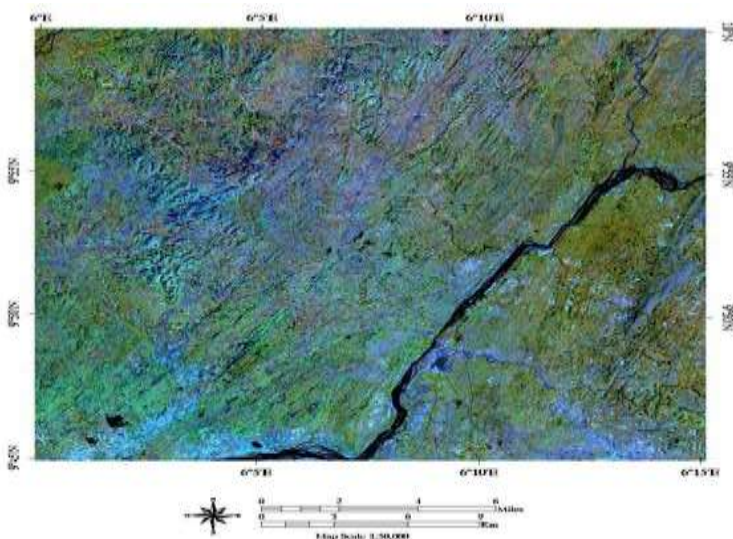


Fig. 5: False colour composite image for bands 5/1, 5/7, 4 displayed in R.G.B

4.3 PRINCIPAL COMPONENT ANALYSIS (PCA)

PCA is a powerful method for analyzing correlated multidimensional data, and many researchers have explored its applications in digital remote sensing (Kaneko, 1978; Byrne et al., 1980; Haralick and Fu, 1983). It is a data transformation process for simplifying a dataset by trying to reduce multidimensional datasets to smaller dimensions for analysis and eliminating information redundancy between bands in order to extract the important information from them (Loughlin, 1991; Gomez et al. 2005). PCA improves overall separability while lowering dimensionality, making it ideal for classification with equal number of input and output spectral bands. The first PCA band has the highest percentage of data variation, while the second PCA band has the second greatest percentage of data variance. The last PCA bands appear noisy because they have very little volatility, much of which is attributed to noise in the original spectral data (Sing and Harrison, 1985; Jensen, 2005; Chang et al., 2006). PCA is a popular tool for lithological and alteration mapping in metallogenic provinces (Crosta et al., 2003; Kargi, 2007; Massironi et al., 2008; Moore et al., 2008; Amer et al., 2010).

PCA has the advantage of compressing most information within all bands (expressed by variance) into a significantly smaller number of bands with negligible data loss (Gibson and Power, 2000). PCA data bands are non-correlated and independent, and they are typically easier to process than the source data (Jensen, 1996).

For the visual interpretation of different rock units, the false color composites (FCC) images of principal component bands PC1, PC2, PC3, PC4, and PC5 shown in Red-Green-Blue (RGB) were generated for the study area (Fig. 6 & Fig. 7). This false color composite PC-image was successful in spectral characterization and differentiating the various types of rocks found in this location.

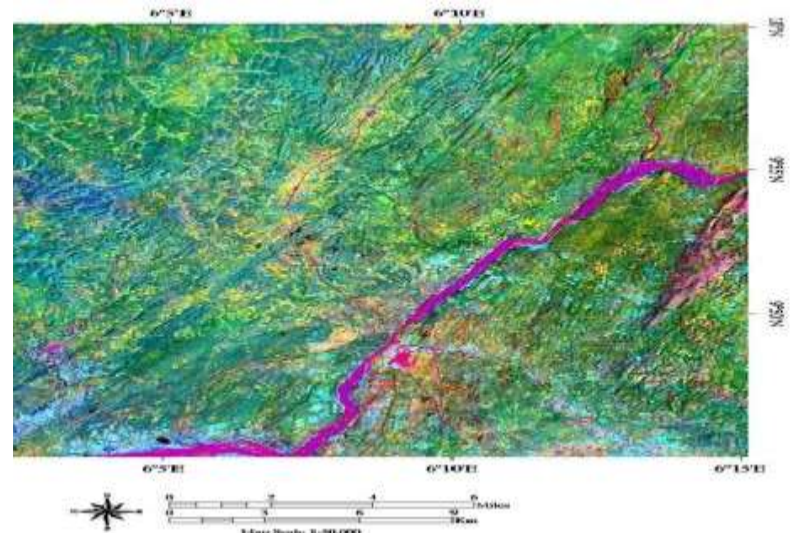


Fig. 6: Principal component analysis of bands 1, 2, 3 displayed in R.G.B

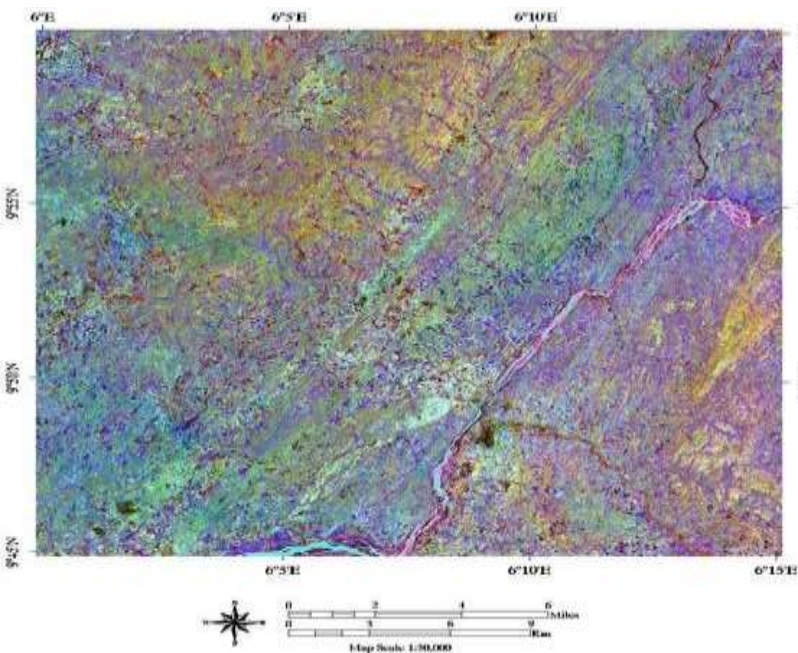


Fig. 7: Principal component analysis of bands 4, 5, 6 displayed in R.G.B

The major drainage system and an amphibolite region in the far eastern portion of the area are indicated by purple colour (Fig. 6). This river appears to be controlled by a major fracture, the Kalangai-Zungeru-Ifewara fault, as it flows through Zungeru. Such large transcurrent fault zones and other minor shear zones are visible on satellite imageries exhibiting a dextral sense of shear. Quartzites, gneisses and schists appear as yellowish-green on the eastern and western portions of the image. The various lithologies and drainage systems exhibit an almost uniform colour in Fig. 7.

4.4 FIELD GEOLOGY AND PETROGRAPHY

The results of Landsat imageries processing have been verified through intensive fieldwork. The lithological units mapped during the field investigation comprise of gneisses, migmatites, quartzites, phyllites, schists, amphibolites and mylonites which are consistent with what (Agbor, 2014) reported. Fresh rock samples from the field were obtained, and representative samples were chosen for petrographic examinations in order to establish their textural and mineralogical makeup.

4.4.1 AMPHIBOLITES

Good exposures of amphibolites are found in river and stream channels in the Eastern and South-Eastern portions of the study area. Some are found along road-cuttings in contact relationship with migmatites. Workers like (Ajibade, Anyanwu and Okoro, 2008) have documented large bodies of amphibolite within the study area. They described the contact between the amphibolites and the quartzo-feldspathic rocks as sharp in some areas while in other areas, the contacts are transitional. Visually in the field, they are black to dark-green in colour (Fig. 8), fine to medium grained in texture and have distinct cleavage planes. Amphibolites appear as purple in the 7,4,1 composite, yellow in the 7,5,4 and blue in the 1/3:5/7:3/5 composite. Principal component 1,2,3 shows the best contrast between this rock and

the surrounding outcrops. The dominant constituents of this metabasic rock are hornblende, plagioclase and quartz. Orthoclase, plagioclase, biotite and augite occur as larger grains, while smaller grain quartz and some plagioclase feldspar form the matrix minerals.



Fig. 8: An amphibolite outcrop found along a fault zone. Location: (9° 47' 31.2" N, 6° 10' 21.7" E)

4.4.2 GARNET MICA SCHIST

These rocks occupy about 10-15% of the entire area mapped predominantly around the Eastern portion of the study area. They are soft, highly weathered and poorly exposed friable rocks (Fig. 9). Intense strain of the parental garnet mica schist has produced a mylonite from this rock in shear zones within the study area. They exhibit same unique colours as Amphibolite in composite 7,4,1 and 7,5,4 in R.G.B.

4.4.3 QUARTZITE

Quartzites are the most common, accounting for around 40% of the rocks in the studied region. Two varieties of quartzite were encountered: the whitish to light brown massive type and the reddish brown, fine to medium grained schistose variety (Fig. 10). Quartzite appears as green in composite 7,4,1 and dark-blue in composite 7,5,4. It exhibits a gradational contact with the gneiss outcrops.



Fig. 9: Photograph of mylonitic garnet mica schists dipping to the west and scattered chunks of cataclastic quartzite all within a shear zone in the study area



Fig. 10: A Photograph of whitish massive quartzite outcrop at Garun Gabas. Location: (9° 51' 25.5" N, 6° 07' 37.5" E)

4.4.4 MIGMATITE

Only a few migmatite exposures have been mapped, mostly in the southeastern portion of the study area. They are rare and concentrated in the southern section of the study area, particularly around Jankwata and Dogon Ruwa (Fig. 13). The migmatites are medium to coarse grained rocks that are distinctively banded and grayish in colour (Fig. 11). Ptygmatic folding occurs in vein-like structure with quartz-filled mineral composition. They are characterized by green and light-yellow in composite 7,4,1 and 7,5,4 respectively similar to the gneiss exposures. PC 4,5,6 (Fig. 7) did not result to any useful map interpretations for this rock type.



Fig. 11: Photograph of a flat-lying Migmatite outcrop around Dogon Ruwa with light and dark bands. Location: (9° 46' 48.0" N, 6° 12' 1.6" E)

4.4.5 GNEISS

This rock covers about 30% of the area mapped. They occur in places like Gulangi, Ushama, Jangaro and Kutuku. Most of the gneisses are highly weathered and breaks easily utilizing foliation planes. Some of the gneisses occur as massive and low lying outcrops especially where they are in contact with the schists. Three different types of gneiss were mapped: (a) an augen gneiss (b) banded gneiss and (c) granitic gneiss. Among these gneisses, the banded gneiss is the most abundant (Fig. 12). Gneiss appears as light purple on composite 7, 4, 1 image and shades of yellow on composite 7, 5, 4. They appear as yellowish-green on PC 1, 2, 3 and do not exhibit a distinct colouration in PC 4, 5, 6 displayed in R.G.B.



Fig. 12: A photograph of banded gneiss north of Zungeru town. Location: (9° 49' 57.9" N, 6° 10' 25.2" E).

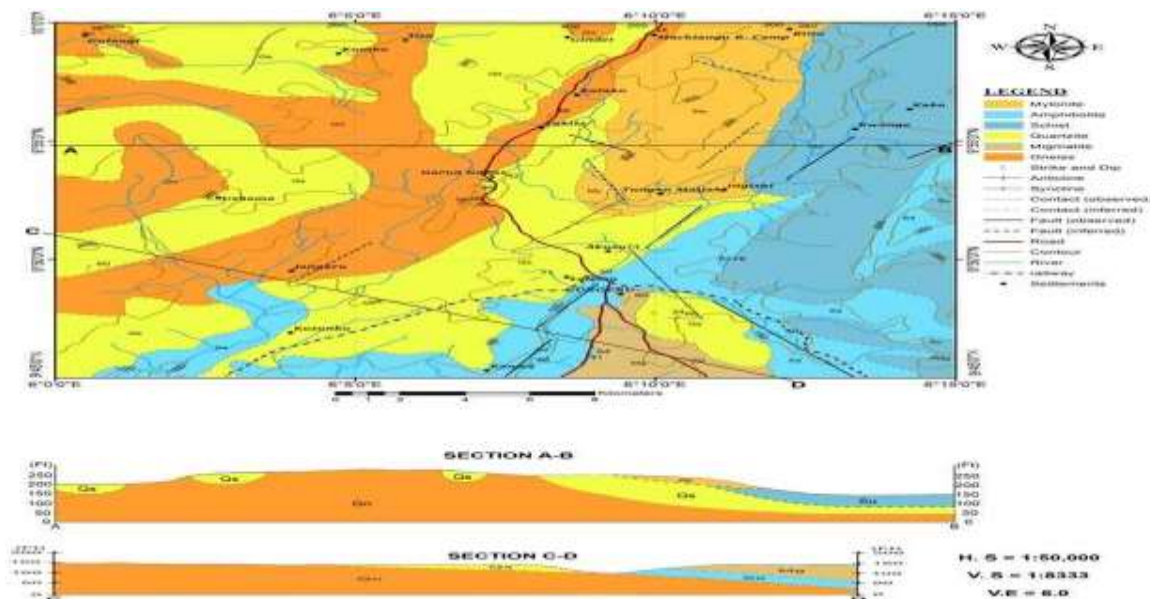


Fig. 13: Geological map and cross-section of the study area

5.0 CONCLUSION

In areas with poor outcrop exposures and inaccessibility as a result of logistical and socio-political constraints, such as part of the Zungeru, field geological mapping is met by a number of setbacks usually in the form of cost, feasibility and security. Because of the synoptic view and the ability to discern distinct lithologies based on their spectral properties, Landsat 7 ETM+ can provide a very useful and low-cost tool for quick mapping in such circumstances.

The rock types encountered in the study area include migmatite-gneisses, schists, amphibolites, quartzites and minor granitic intrusions (Agbor, 2014), but the contact relationship between these rocks is not well defined. In order to differentiate and map the lithologies, certain enhancement techniques such as Principal Component Analysis (PCA), Band Ratio, and False Color Composite techniques were employed on a Landsat 7 ETM+ subset of the Zungeru area in this study. Color composite images created by band rationing and principal component analysis have been especially valuable for visually identifying a variety of rock units within the region.

The most useful images were obtained using a false color composite image for bands 7, 4, 1; 7, 5, 4; and PC 1, 2, 3 presented in R.G.B, emphasizing the small spectral variations between distinct lithological units within the research area. The false color composite of band ratio 1/3:5/7:3/5 and PC 4, 5, 6 exhibited limited enhanced visual display of the rock types. The combination of information derived from these images and fieldwork data aided in the production of a comprehensive and up-to-date geological map which shows clearly the various rock types, their extent and their contact relationships (Fig. 13).

Multispectral remote sensing image enhancement and interpretation of Landsat 7 ETM+ has demonstrated efficacy in lithological rock unit identification and detection. This research shows that, when appropriately processed, low-cost optical

satellite images can be a useful tool for rapid and accurate geologic mapping at a regional scale.

ACKNOWLEDGEMENTS

The authors are grateful to the Global Land Cover Facility (GLCF) at the University of Maryland for providing the Satellite imageries used in conducting this study. We are also thankful to the journal's editors and reviewers for their insightful remarks and ideas.

REFERENCES

- Abdelmalik, K.W., and Abd-Allah, A.M.A., (2018). Integration of remote sensing technique and field data in geologic mapping of an ophiolitic suture zone in western Arabian Shield. *J. Afri. Earth Sci.* 146, 180–190.
- Agbor, A. T.(2014). Geology and Geochemistry of Zungeru Amphibolites, North Central Nigeria, *Universal Journal of Geoscience*, 2(4), 116-122.
- Ajibade, A. C., Anyanwu. N. P. C., Okoro, A. U. (2008). The Geology of Minna Area (explanation of 1:250,000 Sheet 42 (Minna), Nigeria. Geolo. Surv. Agency, Bull. No. 43, 112p.
- Ajibade, A. C., Woakes, M., and Rahaman, M.A. (1987). Proterozoic Crustal Development in the Pan-African Regime of Nigeria. In: C. A. Kogbe (edition) "Geology of Nigeria" 2nd revised edition, *Rock View Nigeria limited, jos*, 57-69.
- Amer, R., Kusky, T., and El Mezayen, A. (2012). Remote sensing detection of gold related alteration zones in Um Rus area, Central Eastern Desert of Egypt. *Advances in Space Research*, 49 (1), 121–134.

- Amer, R., Kusky, T., and Ghulam, A. (2010). Lithological mapping in the Central Eastern Desert of Egypt using ASTER data. *Journal of African Earth Sciences*, **56** (2), 75–82.
- Aminzadeh, B., and Samani, F. (2006). Identifying the boundaries of the historical site of Persepolis using remote sensing. *Remote Sens Environ*, **102**, 52–62.
- Black, R. (1980). Precambrian of West Africa. *Episodes*, **4**, 3-8
- Black, R., Caby R., and Moussine-Pouchkine, A. (1979). Evidence for Late Precambrian Plate Tectonics in West Africa. *Nature*, **278**, 223–226.
- Burke, K.C. and Dewey, J.F., (1972): Orogeny in Africa. In: African Geology, T.F.J. Dessauvage and A.J. Whiteman (eds.), *University of Ibadan Press*, pp. 583-608.
- Byrne, G.F., Crapper, P.F., and Mayo, K. (1980). "Monitoring land cover change by principle component analysis of multitemporal landsat data," *Remote Sensing of Environment*, **10**, 175-189.
- Caby, R., Bertrand, J.M.L., and Black, R., (1981). Pan-African Ocean Closure and Continental Collision in the Hoggar-Iforas Segment, Central Sahara. In: A Kronaer edition, "Precambrian Plate Tectonics" *Elsavier, Amsterdam*, 407-434
- Chang, Q., Jing, L., and Panahi, A. (2006). "Principal Component analysis with optimum order sample correlation coefficient for image enhancement, *International Journal for Remote Sensing*, **27**, 3387-3401.
- Chorowicz, J., and Rangin, C. (1982). Essai de catographie géologique de la basse californie obtenue à partie de l'analyse des images spatiales methods et resultants. *Bull. Soc. Geol. Fr.* **7**, T XXIV, (1) 139-143.
- Crosta, A.P., De Souza Filho, C.R., Azevedo, F. and Brodie, C. (2003). Targeting key alteration minerals in epithermal deposits in Patagonia, Argentina, using ASTER imagery and principal component analysis. *International Journal of Remote Sensing*, **24**, 4233-4240.
- Dada, S.S. (1998). Crust-forming ages and Proterozoic crustal evolution in Nigeria: a reappraisal of current interpretations. *Precambrian Research*, **87**, 65-74.
- Dada, S.S. (2008). Proterozoic Evolution of the Nigeria-Borborema Province," In: R. J. Pankhurst, R. A. Trouw, B. B. Brito Neves and M. J. De Wit, Eds., *West Gondwana: Pre-Cenozoic Correlations across the South Atlantic Region*, *Geological Society of London Special Publication*, London, 121-136
- Danbatta, U.A. (2008). A Review of the Evolution and Tectonic Framework of the Schist Belts of Western Nigeria, West Africa. *Africa geoscience review*, **15** (2), 145-158.
- Ferradini, J., Cornee, J.J., and Simon, B. (1993). Etude linéaire sur images Landsat 2 du Haut Atlas occidental (Maroc): conséquences Géodynamica. *Acta*, **6**, (3), 161-173.
- Gad, S., and Kusky, T.M. (2007). ASTER spectral rationing for lithological mapping in the Arabian-Nubian shield, the Neoproterozoic Wadi Kid area, Sinai, Egypt. *Gondwana Res.* **11** (3), 326–335.
- Galvão Le'nio Soares, Raimundo Almeida-Filho, I'caro Vitorello (2005). Spectral discrimination of hydrothermally altered materials using ASTER short-wave infrared bands: Evaluation in a tropical savannah environment. *Int J Appl Earth Observation Geoinformation*, **7**, 107–114.
- Garba, I. (2002). Late Pan-African Tectonics and Origin of Gold Mineralization and Rare Metals Pegmatites in the Kushaku Schist Belt, *North Western Nigeria. Journal of Mineralogy and Geology*. **3**(1), 1-12.
- Gibson, P. J. and Power, C. H. (2000). *Introductory Remote Sensing: Digital Image Processing and Applications*, Taylor & Francis, Inc., pp. 58-63.
- Gomez, C., Delacourt C., Allemand, P., Ledru, P., and Wackerle, R. (2005). Using ASTER remote sensing data set for geological mapping in Namibia. *Physics and Chemistry of the Earth*, **30**, pp. 97–108.
- Grant, N.K. (1970). Geochronology of Precambrian Basement Rocks from Ibadan, southwestern Nigeria. *Earth and Planetary Science Letters*, **10**, 29-38
- Haralick, R.M., and Fu, K. (1983). "Pattern recognition and classification. In: Colwell RN (ed) *Manual of Remote sensing*," Am Society of Photogrammetry and Remote Sensing, 793-805.
- Hellman, M.J., and Ramsey, M.S. (2004). Analysis of hot springs and associated deposits in Yellowstone National Park using ASTER and AVIRIS remote sensing. *J. Volcanol Geotherm Res* **135**, 195–219.
- Jensen, J. R. (1996). *Introductory Digital Image Processing: A Remote Sensing Perspective*. 2d ed., Englewood Cliffs, New Jersey: Prentice-Hall.
- Jensen, J.R. (2005). "Introductory Digital Image Processing," 3rd edition, Pearson Prentice Hall, 526.
- Kaneko, T. (1978). "Colour composite pictures from principal axis components of multispectral scanner data," *IBM Journal of Research and Development*, **22**, 386-392.
- Kargi, H. (2007). "Principal components analysis for borate mapping," *International Journal for Remote Sensing*, **28**, 8, 1805-1817.
- Kröner, A., Ekwueme, B.N. and Pidgeon, R.T. (2001). The Oldest Rocks in West Africa: SHRIMP Zircon Age for Early Achean Migmatitic Orthogneiss at Kaduna, Northern Nigeria. *Journal of Geology*, university of Chicago, **19**, 399-406.
- Kucukkaya, A.G. (2004). Photogrammetry and remote in archeology. *J Quant Spectroscopy Radiative Transf.*, **88**, 83–88.
- Lammoglia, T., and Filho, C.R.S. (2011). Spectroscopic characterization of oils yielded from Brazilian offshore basins: Potential applications of remote sensing. *Remote Sens Environ*, **115**, 2525–2535.

- Leblanc, M. (1981). The late Proterozoic ophiolites of BouAzzer (Morocco): evidence for Pan-African plate tectonics. In: Kroner, A., (ed.) Precambrian plate tectonics, *Elsevier Amsterdam*, 435-451.
- Loughlin, W. P. (1991). Principal Component Analysis for alteration mapping. *Photogrammetric Engineering and Remote Sensing*, **57**, pp.1163-1169.
- Massironi, M.L., Bertoldi, P., Calafa, D., Visona, A., Bistacchi, C., Giardino, A., and Schiavo, B. (2008). Interpretation and processing of ASTER data for geological mapping and granitoids detection in the Sagro massif (eastern Anti-Atlas, Morocco *Geosphere*, **4** (4), 736–759.
- Moore, F., Rastmanesh, F., Asady, H., and Modabberi, S. (2008). "Mapping mineralogical alteration using principal component analysis and matched filter processing in Takab area, north-west Iran, from ASTER data," *International Journal for Remote Sensing*, **29**, 10, 2851-2867.
- Petrovic, A., Khan, S.D., and Thurmond, A.K. (2012) Integrated hyperspectral remote sensing, geochemical and isotopic studies for understanding hydrocarbon-induced rock alterations. *Mar Pet Geol*, **35**, 292–308.
- Qari, M.H.T., Madani, A.A., Matsah, M.I.M., and Hamimi, Z. (2008). Utilization of Aster and Landsat data in geologic mapping of basement rocks of Arafat area, Saudi Arabia. *The Arabian Journal for Science and Engineering*, **33**, 99-116.
- Raines, G. L., Offield, T.W. and Santos, E.S. (1978). Remote sensing and subsurface definition of facies and structure related to uranium deposits Powder River Basin, Wyoming. *Economic Geology*, **75**, 1706-1725.
- Riley, D.N., Barton, M. and Dalton-Sorrell, C. (2006). Fusion of Landsat-5 thematic mapper and shuttle imaging RADAR-C data for geological mapping in Eastern Maine, USA. Available at: www.gis.usu.edu/docs/protected/procs/asps/asprs2000/pdffiles/papers/222.pdf (accessed November 2006, verified July 2007).
- Rowan, L.C., Wetlaufer, P.H., Goetz, A.F.H., Billingsley, F.C., Stewart, J.H., (1974). Discrimination of rock types and detection of hydrothermally altered areas in south central Nevada by the use of computer-enhanced ERTS images. *U.S. Geological Survey Prof. Pap.* 883, 35.
- Sabins, F. (1997). *Remote Sensing: Principles and Interpretation*, (3rd Ed), 494 p
- Shi, P., Fu, B., Ninomiya, Y., Sun, J., and Li, Y. (2012). Multispectral remote sensing mapping for hydrocarbon seepage-induced lithologic anomalies in the Kuqa foreland basin, south Tian Shan. *J Asian Earth Sci*, **46**, 70–77
- Singh, A., and Harrison, A. (1985). "Standardized principal components," *International Journal for Remote Sensing*, **6**, 883-896.
- Turner, D. C. (1983). Upper Proterozoic Schist Belts in the Nigerian Sector of the Pan-African Province of West-Africa. In: C. A. Kogbe "Geology of Nigeria" 2nd Revised Edition, Rock View Publication Company, Jos, Nigeria. 93-109.
- Van Ruitenbeek, F.J.A., Cudahy, T.J., Van der Meer, F.D., and Hale, M. (2012). Characterization of the hydrothermal systems associated with Archean VMS - mineralization at Panorama, Western Australia, using hyperspectral, geochemical and geothermometric data. *Ore geology reviews*, **45**, 33–46.
- Vaughan, R.G., Hook, S.J., Calvin, W.M., and Taranik, J.V. (2005). Surface mineral mapping at Steamboat Springs, Nevada, USA, with multi-wavelength thermal infrared images, *Remote Sens Environ*, **99**, 140–158.
- Watts, D.R. and Harris, N.B.W. (2005). Mapping granite and gneiss in domes along the North Himalayan antiform with ASTER SWIR band ratios. *Geol Soc Am Bull.* 117(7/8):879–886.
- Zhang, X., Pazner, M., and Duke, N. (2007). Lithologic and mineral information extraction for gold exploration using ASTER data in the south Chocolate Mountains (California). *ISPRS Journal of Photogrammetry and Remote Sensing*, **62** (4), 271–282.



©2021 This is an Open Access article distributed under the terms of the Creative Commons Attribution 4.0 International license viewed via <https://creativecommons.org/licenses/by/4.0/> which permits unrestricted use, distribution, and reproduction in any medium, provided the original work is cited appropriately.